Alexandria Engineering Journal (2015) 54, 45–54

Alexandria University

Alexandria Engineering Journal

www.elsevier.com/locate/aej
www.sciencedirect.com

ORIGINAL ARTICLE

Numerical/Laplace transform analysis for MHD radiating heat/mass transport in a Darcian porous regime bounded by an oscillating vertical surface

Sahin Ahmed [*,a], **Abdul Batin** [b], **A.J. Chamkha** [c]

[a] *Heat Transfer and Fluid Mechanics Research, Department of Mathematics and Computing, Rajiv Gandhi University, Rono Hills 791112, Arunachal Pradesh, India*
[b] *Department of Mathematics, Indira Gandhi College, Boitamari, Bongaigaon 783389, Assam, India*
[c] *Manufacturing Engineering Department, The Public Authority for Applied Education and Training, Shuweikh 70654, Kuwait*

Received 8 April 2014; revised 19 November 2014; accepted 23 November 2014
Available online 13 December 2014

KEYWORDS

Crank–Nicolson;
Absorbing/emitting radiation;
Darcian porosity;
Shear stress;
Materials processing;
Boussinesq's approximation

Abstract Analytical and numerical solutions of a non-linear MHD flow with heat and mass transfer characteristics of an incompressible, viscous, electrically conducting and Boussinesq's fluid over a vertical oscillating plate embedded in a Darcian porous medium in the presence of thermal radiation effect have been presented. The fluid considered here is gray, absorbing/emitting radiating, but non-scattering medium. At time $t > 0$, the plate temperature and concentration near the plate raised linearly with time t. The dimensionless governing coupled, non-linear boundary layer partial differential equations are solved by an efficient, accurate, extensively validated and unconditionally stable finite difference scheme of the Crank–Nicolson type as well as by the Laplace Transform technique. An increase in porosity parameter (K) is found to depress fluid velocities and shear stress in the regime. Also it has been found that, when the conduction-radiation (R) increased, the fluid velocity and the temperature profiles decreased. Applications of the study arise in materials processing and solar energy collector systems.

1. Introduction

In recent years, the problems of free convective and heat transfer flows through a porous medium under the influence of a magnetic field have been attracted the attention of a number of researchers because of their possible applications in many branches of science and technology, such as its applications in transportation cooling of re-entry vehicles and rocket boosters, cross-hatching on ablative surfaces and film vaporization in combustion chambers. On the other hand, flow through a porous medium has numerous engineering and geophysical applications, such as, in the chemical engineering filtration and purification process; in the agricultural engineering, to study the underground water resources; in the petroleum

* Corresponding author. Tel.: +91 9435024242.
E-mail addresses: asahinrgu@gmail.com (S. Ahmed), abdulbatin@yahoo.in (A. Batin), achamkha@yahoo.com (A.J. Chamkha).
Peer review under responsibility of Faculty of Engineering, Alexandria University.

http://dx.doi.org/10.1016/j.aej.2014.11.006

Nomenclature

$(\bar{u}, \bar{v})$	velocity components along $(\bar{x}, \bar{y})$-directions
U_0	dimensionless plate velocity (m s^{-1})
$\bar{a}$	spectral mean absorption coefficient of the medium
C_P	specific heat at constant pressure (J kg^{-1} K)
g	acceleration due to gravity (m s^{-2})
Gr	thermal Grashoff number
Gr_m	mass Grashoff number
K	permeability of the porous medium
M	Hartmann number
Pr	Prandtl number
q_r	radiative heat flux
R	radiation-conduction parameter
$\overline{T}$	temperature (K)
$\overline{T}_w$	fluid temperature at the surface (K)
$\overline{T}_\infty$	fluid temperature in the free stream (K)
$\overline{C}$	concentration (kg m^{-3})
$\overline{C}_w$	concentration at the surface (kg m^{-3})
$\overline{C}_\infty$	concentration in the free stream (kg m^{-3})
Sc	Schmidt number
D	molecular diffusivity
t	dimensionless time
u	dimensionless velocity component in x-direction (m s^{-1})
v	dimensionless velocity component in y-direction (m s^{-1})

Greek symbols

β	coefficient of volume expansion for heat transfer (K^{-1})
κ	thermal conductivity (W m^{-1} K^{-1})
θ	dimensionless fluid temperature (K)
ϕ	dimensionless concentration (kg m^3)
ρ	density (kg m^{-3})
σ	electrical conductivity
$\bar{\sigma}$	Stefan–Boltzmann constant
τ_x	shearing stress (N m^{-2})
υ	kinematic viscosity (m^2 s^{-1})

Subscripts

w	conditions on the wall
∞	free stream conditions

technology, to study the movement of natural gas, oil and water through the oil reservoirs. In view of these applications, many researchers have studied MHD free convective heat and mass transfer flow in a porous medium with different configurations; some of them are Raptis and Kafoussias [1], Sattar [2] and Kim [3]. Jaiswal and Soundalgekar [4] obtained an approximate solution to the problem of an unsteady flow past an infinite vertical plate with constant suction and embedded in a porous medium with oscillating plate temperature. The unsteady flow through a highly porous medium in the presence of radiation was studied by Raptis and Perdikis [5]. Ahmed [6] investigated the effect of transverse periodic permeability oscillating with time on the heat transfer flow of a viscous incompressible fluid through a highly porous medium bounded by an infinite vertical porous plate, by means of series solution method. Ahmed [7] studied the effect of transverse periodic permeability oscillating with time on the free convective heat transfer flow of a viscous incompressible fluid through a highly porous medium bounded by an infinite vertical porous plate subjected to a periodic suction velocity. Kumar and Verma [8] presented the problem of an unsteady flow past an infinite vertical permeable plate with constant suction and transverse magnetic field with oscillating plate temperature.

If temperature of the surrounding fluid is high, radiation effects play an important role and this situation does not exist in space technology. In such cases one has to take into account the effect of thermal radiation and mass diffusion. The effects of radiation and viscous dissipation on the transient natural convection-radiation flow of viscous dissipation fluid along an infinite vertical surface embedded in a porous medium, by means of network simulation method, investigated by Zueco [9]. The effect of radiation on natural convection flow of a Newtonian fluid along a vertical surface embedded in a porous medium has presented by Mahmoud and Chamkha [10]. Soundalgekar and Takhar [11] have considered the radiation free convection flow of an optically thin gray gas past a semi-infinite vertical plate. Radiation effects on mixed convection flow along an isothermal vertical plate were studied by Hossain and Takhar [12]. In all the above studies, the vertical plate has been considered as stationary. Raptis and Perdikis [13] studied the effects of thermal radiation and free convection flow past a moving vertical plate. The governing equations were solved analytically. Ahmed [14] studied effects of radiation and magnetic Prandtl number on the steady mixed convective heat and mass transfer flow of an optically thin gray gas over an infinite vertical porous plate with constant suction in presence of transverse magnetic field. Ahmed [15] investigated the effects of radiation and viscous dissipation heat on a magnetohydrodynamic steady mixed convective heat and mass transfer flow over an infinite vertical porous plate with constant suction taking into account the induced magnetic field. Ahmed and Kalita [16] investigated the effects of porosity and magnetohydrodynamic on a horizontal channel flow of a viscous incompressible electrically conducting fluid through a porous medium in the presence of thermal radiation and transverse magnetic field. Ahmed and Kalita [17] presented the magnetohydrodynamic transient convective radiative heat transfer in an isotropic, homogenous porous regime adjacent to a hot vertical plate. Ahmed and Kalita [18] investigated the effects of chemical reaction as well as magnetic field on the heat and mass transfer of Newtonian fluids over an infinite vertical oscillating plate with variable mass diffusion. Ahmed et al. [19] gave a numerical solution for the problem of magnetohydrodynamic heat and mass transfer flow past an impulsively started semi-infinite vertical plate in the presence of thermal radiation by an implicit finite-difference scheme of

Crank–Nicolson type. The effects of Darcian drag force and radiation-conduction on the unsteady two-dimensional magnetohydrodynamic flow of a viscous, electrically conducting and Newtonian fluid over a vertical plate adjacent to a Darcian regime in the presence of thermal radiation and transversal magnetic field were reported by Ahmed et al. [20]. Ahmed [21] analyzed the effects of conduction-radiation, porosity and chemical reaction on the unsteady hydromagnetic free convection flow past an impulsively-started semi-infinite vertical plate embedded in a porous medium in the presence of first order chemical reaction and thermal radiation. The boundary layer equations have been solved by an implicit finite-difference scheme of the Crank–Nicolson type, which is efficient, accurate, extensively validated and unconditionally stable.

Kumar [23] investigated a new approximate method, namely homotopy perturbation transform method (HPTM) which is a combination of homotopy perturbation method (HPM) and Laplace transform method (LTM) to provide an analytical approximate solution to time-fractional Cauchy-reaction diffusion equation. The problem of a non-Newtonian plane Couette flow, fully developed plane Poiseuille flow and Couette–Poiseuille flow was presented by Ellahi and Hameed [24]. The effects of heat and mass transfer with slip on the Couette and generalized Couette flow in a homogeneous and thermodynamically compatible third grade non-Newtonian viscous fluid and the exact solutions of velocity and temperature in Couette flow problem were derived by Ellahi et al. [25]. Ahmed et al. [26] studied the oscillatory hydromagnetic flow of a viscous, incompressible, electrically-conducting, non-Newtonian fluid in an inclined, rotating channel with non-conducting walls, incorporating couple stress effects. Zueco et al. [27] investigated the 2D steady-state boundary layer flow and heat transfer of an electrically conducting incompressible micropolar fluid over a continuously moving stretching surface embedded in a Darcian porous medium with a uniform magnetic field imposed in the direction normal to the surface and the stretching velocity is assumed to vary linearly with the distance along the sheet. Ibrahim et al. [28] analyzed the effects of radiation absorption, mass diffusion, chemical reaction and heat source parameter of heat generating fluid past a vertical porous plate subjected to variable suction and it has assumed that the plate is embedded in a uniform porous medium and moves with a constant velocity in the flow direction in the presence of a transverse magnetic field. The influence of thermal radiation and first-order chemical reaction on unsteady MHD convective flow, heat and mass transfer of a viscous incompressible electrically conducting fluid past a semi-infinite vertical flat plate in the presence of transverse magnetic field under oscillatory suction and heat source in slip-flow regime were studied by Pal and Talukdar [29].

In this paper, the effects of porosity of the porous medium and radiation-conduction on the heat and mass transfer of Newtonian fluids over an infinite vertical oscillating permeable plate immersed in a saturated porous medium with variable mass diffusion have considered. The external magnetic field is applied transversely to the vertical plate. The temperature and concentration of the plate is oscillating with time about a constant non-zero mean value. The conservation equations are normalized and then solved using both the Laplace Transform technique and stable finite difference scheme of the Crank–Nicolson type. Excellent agreement has obtained between analytical and numerical methods.

2. Mathematical analysis

Unsteady MHD laminar boundary-layer flow of a viscous incompressible Newtonian fluid past along a vertical oscillating plate embedded in a saturated porous medium with variable temperature and also with mass diffusion in the presence of transverse applied magnetic field and thermal radiation has been considered in Fig. 1. The $\bar{x}$ axis is taken along the plate in the vertical upward direction and the $\bar{y}$ axis is taken normal to the plate. Initially it is assumed that the plate and fluid are at the same temperature $\overline{T}_\infty$ in the stationary condition with concentration level $\overline{C}_\infty$ at all the points. At time, $\bar{t} > 0$ the plate is given an oscillatory motion in its own plane with velocity $U_0 \cos(\bar{\omega}\bar{t})$. At the same time the plate temperature is raised linearly with time $\bar{t}$ and also mass is diffused from the plate linearly with time. A transverse magnetic field of uniform strength B_0 is assumed to be applied normal to the plate. As the magnetic Reynolds number of the flow is taken very small, the *induced* magnetic field and viscous dissipation are assumed to be negligible. The fluid considered here is gray, absorbing/emitting radiation but a non-scattering medium. Then by usual Boussinesq's approximation, the unsteady flow is governed by the following equations:

$$\frac{\partial \bar{u}}{\partial \bar{t}} = g\beta(\overline{T} - \overline{T}_\infty) + g\bar{\beta}(\overline{C} - \overline{C}_\infty) + \nu \frac{\partial^2 \bar{u}}{\partial \bar{y}^2} - \left(\frac{\sigma B_0^2}{\rho} + \frac{\nu}{\overline{K}}\right)\bar{u}, \quad (1)$$

$$\rho C_P \frac{\partial \overline{T}}{\partial \bar{t}} = \kappa \frac{\partial^2 \overline{T}}{\partial \bar{y}^2} - \frac{\partial q_r}{\partial \bar{y}}, \quad (2)$$

$$\frac{\partial \overline{C}}{\partial \overline{T}} = D \frac{\partial^2 \overline{C}}{\partial \bar{y}^2}. \quad (3)$$

The initial and boundary conditions are as follows:

$$\left.\begin{array}{l} \bar{t} \leqslant 0 : \bar{u} = 0, \quad \overline{T} = \overline{T}_\infty, \quad \overline{C} = \overline{C}_\infty \quad \forall y \\ \bar{t} > 0 : \bar{u} = U_0 \cos(\bar{\omega}\bar{t}), \quad \overline{T} = \overline{T}_\infty + (\overline{T}_w - \overline{T}_\infty)A\bar{t}, \\ \overline{C} = \overline{C}_\infty + (\overline{C}_w - \overline{C}_\infty)A\bar{t} \text{ at } y = 0 \\ \bar{t} > 0 : \bar{u} \to 0, \quad \overline{T} \to \overline{T}_\infty, \quad \overline{C} \to \overline{C}_\infty \text{ as } y \to \infty. \end{array}\right\} \quad (4)$$

The local radiant absorption for the case of an optically thin gray gas is expressed as

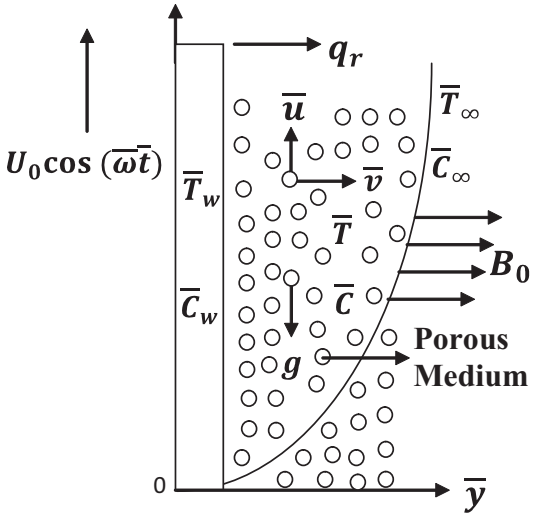

Figure 1 Physical configuration and coordinate system.

$$\frac{\partial q_r}{\partial \bar{y}} = -4\bar{a}\bar{\sigma}\left(\overline{T}_\infty^4 - \overline{T}^4\right), \tag{5}$$

where $\bar{\sigma}$ and $\bar{a}$ are the Stefan–Boltzmann constant and the Mean absorption coefficient, respectively. Following Raptis–Perdikis [5] and Ahmed [14,15] and others, we assume that the temperature differences within the flow are sufficiently small so that $\overline{T}^4$ can be expressed as a linear function of $\overline{T}$ after using Taylor's series to expand $\overline{T}^4$ about the free stream temperature $\overline{T}_\infty$ and neglecting higher-order terms. This results in the following approximation:

$$\overline{T}^4 \cong 4\overline{T}_\infty^3\overline{T} - 3\overline{T}_\infty^4, \tag{6}$$

$$\rho C_P\frac{\partial \overline{T}}{\partial \bar{t}} = \kappa\frac{\partial^2\overline{T}}{\partial \bar{y}^2} - 16\bar{a}\bar{\sigma}\overline{T}_\infty^3(\overline{T} - \overline{T}_\infty). \tag{7}$$

Introducing the following non-dimensional quantities

$$\begin{aligned} &y = \frac{v_0\bar{y}}{v}, \quad u = \frac{\bar{u}}{u_0}, \quad \theta = \frac{\overline{T} - \overline{T}_\infty}{\overline{T}_w - \overline{T}_\infty}, \quad \phi = \frac{\overline{C} - \overline{C}_\infty}{\overline{C}_w - \overline{C}_\infty},\\ &Sc = \frac{v}{D}, \quad Pr = \frac{\rho v C_P}{\kappa}, \quad K_r = \frac{u_0^2\bar{K}}{v^2}, \quad A = \frac{u_0^2}{v}\\ &Gr = \frac{vg\beta(\overline{T}_w - \overline{T}_\infty)}{u_0^3}, \quad Gr_m = \frac{vg\bar{\beta}(\overline{C}_w - \overline{C}_\infty)}{u_0^3},\\ &t = \frac{u_0^2\bar{t}}{v}, \quad M = \frac{\sigma B_0^2 v}{\rho u_0^2}, \quad R = \frac{16\bar{a}v\bar{\sigma}\overline{T}_\infty^3}{\kappa u_0^2}. \end{aligned} \tag{8}$$

Using the transformations (8), the non-dimensional forms of (1), (3) and (7) are

$$\frac{\partial u}{\partial t} = \frac{\partial^2 u}{\partial y^2} - \left(M + K_r^{-1}\right)u + Gr\theta + Gr_m\phi, \tag{9}$$

$$\frac{\partial \theta}{\partial t} = \frac{1}{Pr}\frac{\partial^2\theta}{\partial y^2} - \frac{R}{Pr}\theta, \tag{10}$$

$$\frac{\partial \phi}{\partial t} = \frac{1}{Sc}\frac{\partial^2\phi}{\partial y^2}. \tag{11}$$

The corresponding initial and boundary conditions are

$$\left.\begin{aligned} &t \leqslant 0 : u = 0, \quad \theta = 0, \quad \phi = 0 \quad \forall y\\ &t > 0 : u = \cos(\omega t), \quad \theta = t, \quad \phi = t \quad \text{at } y = 0\\ &t > 0 : u \to 0, \quad \theta \to 0, \quad \phi \to 0 \text{ as } y \to \infty \end{aligned}\right\}. \tag{12}$$

3. Method of solution

The unsteady, non-linear, coupled partial differential Eqs. (9)–(11) along with their boundary conditions (12) have been solved analytically using usual Laplace transform technique and the solutions for hydromagnetic flow in the presence of radiation and porosity of the medium are obtained as follows:

$$\begin{aligned} \theta(y,t) = &\left(\frac{t}{2} + \frac{yPr}{4\sqrt{R}}\right)\exp\left(y\sqrt{R}\right)erfc\left(\eta\sqrt{Pr} + \sqrt{\frac{Rt}{Pr}}\right)\\ &+ \left(\frac{t}{2} - \frac{yPr}{4\sqrt{R}}\right)\exp\left(-y\sqrt{R}\right)erfc\left(\eta\sqrt{Pr} - \sqrt{\frac{Rt}{Pr}}\right), \end{aligned} \tag{13}$$

$$\phi(y,t) = t\left[\left(1 + 2\eta^2 Sc\right)erfc\left(\eta\sqrt{Sc}\right) - \frac{2\eta\sqrt{Sc}}{\sqrt{\pi}}\exp\left(-\eta^2 Sc\right)\right], \tag{14}$$

$$\begin{aligned} u(y,t) = &\frac{1}{4}\exp(i\omega t)\left[\exp\left(y\sqrt{N + i\omega}\right)erfc\left\{\eta + \sqrt{(N + i\omega)t}\right\}\right.\\ &\left.+\exp\left(-y\sqrt{N + i\omega}\right)erfc\left\{\eta - \sqrt{(N + i\omega)t}\right\}\right]\\ &+\frac{1}{4}\exp(-i\omega t)\left[\exp\left(y\sqrt{N - i\omega}\right)erfc\left\{\eta + \sqrt{(N - i\omega)t}\right\}\right.\\ &\left.+\exp\left(-y\sqrt{N - i\omega}\right)erfc\left\{\eta - \sqrt{(N - i\omega)t}\right\}\right]\\ &-\frac{A}{2}\left[\exp\left(y\sqrt{N}\right)erfc\left(\eta + \sqrt{Nt}\right)\right.\\ &\left.+\exp\left(-y\sqrt{N}\right)erfc\left(\eta - \sqrt{Nt}\right)\right]\\ &+B\left[\left(\frac{t}{2} + \frac{y}{4\sqrt{N}}\right)\exp\left(y\sqrt{N}\right)erfc\left(\eta + \sqrt{Nt}\right)\right.\\ &\left.+\left(\frac{t}{2} - \frac{y}{4\sqrt{N}}\right)\exp(-y\sqrt{N})erfc\left(\eta - \sqrt{Nt}\right)\right]\\ &+\frac{E}{2}\exp(-Ct)\left[\exp\left(y\sqrt{N - C}\right)erfc\left\{\eta + \sqrt{(N - C)t}\right\}\right.\\ &\left.+\exp\left(-y\sqrt{N - C}\right)erfc(\eta - \sqrt{(N - C)t}\right]\\ &+\frac{G}{2}\exp(et)\left[\exp\left(y\sqrt{N + e}\right)erfc\left\{\eta + \sqrt{(N + e)t}\right\}\right.\\ &\left.+\exp\left(-y\sqrt{N + e}\right)erfc\eta - \sqrt{(N + e)t}\right]\\ &+\frac{E}{2}\left[\exp\left(y\sqrt{R}\right)erfc\left(\eta\sqrt{Pr} + \sqrt{\frac{Rt}{Pr}}\right)\right.\\ &\left.+\exp\left(-y\sqrt{R}\right)erfc\left(\eta\sqrt{Pr} - \sqrt{\frac{Rt}{Pr}}\right)\right] + D\theta(y,t) + F\phi(y,t)\\ &+\frac{E}{2}\exp(-Ct)\left[\exp\left(y\sqrt{R - CPr}\right)erfc\left\{\eta\sqrt{Pr} + \sqrt{\left(\frac{R}{Pr} - C\right)t}\right\}\right.\\ &\left.+\exp\left(-y\sqrt{R - CPr}\right)erfc\left\{\eta\sqrt{Pr} - \sqrt{\left(\frac{R}{Pr} - C\right)t}\right\}\right]\\ &+G\,erfc\left(\eta\sqrt{Sc}\right) - \frac{G}{2}\left[\exp\left(y\sqrt{eSc}\right)erfc\left(\eta\sqrt{Sc} + \sqrt{et}\right)\right.\\ &\left.+\exp\left(-y\sqrt{eSc}\right)erfc\left(\eta\sqrt{Sc} - \sqrt{et}\right)\right]. \end{aligned} \tag{15}$$

where $\eta = \dfrac{y}{2\sqrt{t}}$, $N = M + K_r^{-1}$,

$$A = \frac{Gr(Pr - 1)}{(R - N)^2} + \frac{Gr_m(Sc - 1)}{N^2},$$

$$B = \frac{N(Gr + Gr_m) - RGr_m}{N(R - N)}, \quad C = \frac{R - N}{Pr - 1}, \quad D = \frac{Gr}{R - N},$$

$$e = \frac{N}{Sc - 1}, \quad E = \frac{Gr(Pr - 1)}{(R - N)^2}, \quad F = \frac{Gr_m}{N},$$

$$G = Gr_m\left(\frac{Sc - 1}{N}\right)^2.$$

4. Skin friction

The boundary layer produces a drag force on the plate due to the viscous stresses which are developed at the wall. The viscous stress at the surface of the plate is given by

$$\tau = -\left[\frac{\partial u(y,t)}{\partial y}\right]_{y=0} = -\frac{1}{2\sqrt{t}}\left[\frac{\partial u(y,t)}{\partial \eta}\right]_{\eta=0}$$
$$= \frac{1}{2}\exp(i\omega t)\left[\frac{\exp\{-(N+i\omega)t\}}{\sqrt{\pi t}} + \sqrt{N+i\omega}\, erf\left\{\sqrt{(N+i\omega)t}\right\}\right]$$
$$+ \frac{1}{2}\exp(-i\omega t)\left[\frac{\exp\{-(N-i\omega)t\}}{\sqrt{\pi t}} + \sqrt{N-i\omega}\, erf\left\{\sqrt{(N-i\omega)t}\right\}\right]$$
$$- A\left[\frac{1}{\sqrt{\pi t}}\exp(-Nt) + \sqrt{N}erf\left(\sqrt{Nt}\right)\right]$$
$$+ B\left[\sqrt{\frac{t}{\pi}}\exp(-Nt) + \left(t\sqrt{N} + \frac{1}{2\sqrt{N}}\right)erf\left(\sqrt{Nt}\right)\right]$$
$$+ E\exp(-Ct)\left[\frac{1}{\sqrt{\pi t}}\exp\{-(N-C)t\}\right.$$
$$\left. + \sqrt{N-C}\, erf\left\{\sqrt{(N-C)t}\right\}\right] + G\exp(et)\left[\frac{1}{\sqrt{\pi t}}\exp\{-(N+e)t\}\right.$$
$$\left. + \sqrt{N+e}\, erf\left\{\sqrt{(N+e)t}\right\}\right] + E\left[\sqrt{\frac{Pr}{\pi t}}\exp\left(\frac{-Rt}{Pr}\right)\right.$$
$$\left. + \sqrt{R}erf\left(\sqrt{\frac{Rt}{Pr}}\right)\right] + D\left[t\sqrt{R}erf\left(\sqrt{\frac{Rt}{Pr}}\right) + \sqrt{\frac{tPr}{\pi}}\exp\left(\frac{-Rt}{Pr}\right)\right.$$
$$\left. + \frac{Pr}{2\sqrt{R}}erf\left(\sqrt{\frac{Rt}{Pr}}\right)\right] + E\exp(-Ct)\left[\sqrt{\frac{Pr}{\pi t}}\exp\left\{-\left(\frac{R}{Pr} - C\right)t\right\}\right.$$
$$\left. + \sqrt{R - CPr}erf\left\{\sqrt{\left(\frac{R}{Pr} - C\right)t}\right\}\right] + G\sqrt{\frac{Sc}{\pi t}} + 2F\sqrt{\frac{tSc}{\pi}}$$
$$- G\exp(et)\left[\sqrt{\frac{Sc}{\pi t}}\exp(-et) + \sqrt{eSc}\, erf\left(\sqrt{et}\right)\right]. \tag{16}$$

5. Numerical technique

In order to solve the unsteady, non-linear coupled Eqs. (9)–(11) under the conditions (12), an implicit finite difference scheme of the Crank–Nicolson type has been employed. The finite difference equations corresponding to Eqs. (9)–(11) are as follows:

$$\frac{\left[u_{i,j}^{n+1} - u_{i,j}^{n}\right]}{\Delta t} = \frac{1}{2(\Delta y)^2}\left[u_{i,j-1}^{n+1} - 2u_{i,j}^{n+1} + u_{i,j+1}^{n+1} + u_{i,j-1}^{n} - 2u_{i,j}^{n} + u_{i,j+1}^{n}\right]$$
$$+ \frac{Gr\left[\theta_{i,j}^{n+1} + \theta_{i,j}^{n}\right]}{2} + \frac{Gr_m\left[\phi_{i,j}^{n+1} + \phi_{i,j}^{n}\right]}{2}$$
$$- \frac{\left[u_{i,j}^{n+1} + u_{i,j}^{n}\right]}{2}(M + K^{-1}), \tag{17}$$

$$\frac{\left[\theta_{i,j}^{n+1} - \theta_{i,j}^{n}\right]}{\Delta t} = \frac{\left[\theta_{i,j-1}^{n+1} - 2\theta_{i,j}^{n+1} + \theta_{i,j+1}^{n+1} + \theta_{i,j-1}^{n} - 2\theta_{i,j}^{n} + \theta_{i,j+1}^{n}\right]}{2Pr(\Delta y)^2}$$
$$- \frac{R_a\left[\theta_{i,j}^{n+1} + \theta_{i,j}^{n}\right]}{2Pr}, \tag{18}$$

$$\frac{\left[\phi_{i,j}^{n+1} - \phi_{i,j}^{n}\right]}{\Delta t} = \frac{\left[\phi_{i,j-1}^{n+1} - 2\phi_{i,j}^{n+1} + \phi_{i,j+1}^{n+1} + \phi_{i,j-1}^{n} - 2\phi_{i,j}^{n} + \phi_{i,j+1}^{n}\right]}{2Sc(\Delta y)^2}, \tag{19}$$

The region of integration is considered as a rectangle with sides x_{max}(= 1) and y_{max}(= 14), where y_{max} corresponds to $y = \infty$ which lies in the momentum and energy boundary layers. The maximum of y is chosen as 14 after some preliminary investigations so that the last two of the boundary conditions (14) are satisfied within the tolerance limit 10^{-5}. After experimenting with a few set of mesh sizes, the mesh sizes have been fixed at the level $\Delta y = 0.25$ with time step $t = 0.01$. In this case, the spatial mesh sizes are reduced by 50% in one direction, and later in both directions, and the results are compared. It is observed that, when the mesh size is reduced by 50% in the y-direction, the results differ in the fifth decimal place while the mesh sizes are reduced by 50% in x-direction or in both directions; the results are comparable to three decimal places.

Hence, the above mesh sizes have been considered as appropriate for calculation. The coefficients $u_{i,j}^{n}$ and $v_{i,j}^{n}$ appearing in the finite-difference equations are treated as constants in any one time step. Here i-designates the grid point along the x-direction, j along the y-direction. The values of u, v and θ are known at all grid points at $t = 0$ from the initial conditions.

The computations of u, v, θ and ϕ at time level $(n + 1)$ using the values at previous time level (n) are carried out as follows: The finite difference Eq. (19) at every internal nodal point on a particular i-level constitutes a tridiagonal system of equations. Such systems of equations are solved by using Thomas algorithm as discussed in Carnahan et al. (1969). Thus, the values of ϕ are found at every nodal point for a particular i at $(n + 1)$th time level. Similarly, the values of θ are calculated from Eq. (18). Using the values of ϕ and θ at $(n + 1)$th time level in Eq. (17), the values of u at $(n + 1)$th time level are found in a similar manner. Thus, the values of ϕ, θ and u are known on a particular i-level. This process is repeated for various i-level. Thus the values of ϕ, θ, u are known, at all grid points in the rectangular region at $(n + 1)$th time level.

In a similar manner, computations are carried out by moving along the i-direction. After computing values corresponding to each i at a time level, the values at the next time level are determined in a similar manner. Computations are repeated until the steady-state is reached. The steady state solution is assumed to have been reached, when the absolute difference between the values of u, as well as temperature θ and concentration ϕ at two consecutive time steps are less than 10^{-5} at all grid points.

5.1. Stability analysis

The stability criterion of the finite difference scheme for constant mesh sizes is examined using Von-Neumann technique as explained by Carnahan et al. [22]. The general term of the Fourier expansion for u, θ and ϕ at a time arbitrarily called $t = 0$, is assumed to be of the form $\exp(i\beta y)$ (here $i = \sqrt{-1}$). At a later time t, these terms will become,

$$u = H_1(t)\exp(i\beta y), \quad \theta = H_2(t)\exp(i\beta y),$$
$$\phi = H_3(t)\exp(i\beta y). \tag{20}$$

Substituting Eqs. (20) in Eqs. (17)–(19) under the assumption that the coefficients u, θ and ϕ are constants over any one time step and denoting the values after one time step by H_1', H_2' and H_3'. After simplification, we get

$$\frac{H_1' - H_1}{\Delta t} = \frac{(H_2' + H_2)Gr + (H_3' + H_3)Gr_m}{2} + (H_1' + H_1)\left[\frac{\{\cos(\beta\Delta y) - 1\}}{(\Delta y)^2} - \frac{(M + K^{-1})}{2}\right], \quad (21)$$

$$\frac{H_2' - H_2}{\Delta t} = \left[\frac{\{\cos(\beta\Delta y) - 1\}}{(\Delta y)^2} - \frac{R_a}{2}\right]\frac{(H_2' + H_2)}{Pr}, \quad (22)$$

$$\frac{H_3' - H_3}{\Delta t} = \left[\frac{\{\cos(\beta\Delta y) - 1\}}{(\Delta y)^2}\right]\frac{(H_3' + H_3)}{Sc}. \quad (23)$$

Eqs. (21)–(23) can be rewritten as,

$$(1 + I)H_1' = (1 - I)H_1 + \frac{\Delta t}{2}\left[Gr(H_2' + H_2) + Gr_m(H_3' + H_3)\right], \quad (24)$$

$$(1 + J)H_2' = (1 - J)H_2, \quad (25)$$

$$(1 + L)H_3' = (1 - L)H_3. \quad (26)$$

where $I = [1 - \cos(\beta\Delta y)]\dfrac{\Delta t}{(\Delta y)^2} + \dfrac{(M + K^{-1})\Delta t}{2}$,

$J = [1 - \cos(\beta\Delta y)]\dfrac{\Delta t}{Pr(\Delta y)^2} + \dfrac{R_a\Delta t}{2Pr}$,

$L = [1 - \cos(\beta\Delta y)]\dfrac{\Delta t}{Sc(\Delta y)^2}$.

After eliminating H_2' and H_3' in Eq. (24) using Eqs. (25) and (26), the resultant equation is given by,

$$(1 + I)H_1' = (1 - I)H_1 + H_2\frac{Gr\Delta t}{(1 + J)} + H_3\frac{Gr_m\Delta t}{(1 + L)}. \quad (27)$$

Eqs. (25)–(27) can be written in matrix form as follows:

$$\begin{pmatrix} H_1' \\ H_2' \\ H_3' \end{pmatrix} = \begin{pmatrix} \frac{1-I}{1+I} & P_1 & P_2 \\ 0 & \frac{1-J}{1+J} & 0 \\ 0 & 0 & \frac{1-L}{1+L} \end{pmatrix}\begin{pmatrix} H_1 \\ H_2 \\ H_3 \end{pmatrix}, \quad (28)$$

where $P_1 = \dfrac{Gr\Delta t}{(1 + I)(1 + J)}$ and $P_2 = \dfrac{Gr_m\Delta t}{(1 + I)(1 + L)}$.

Now, for stability of the finite difference scheme, the modulus of each *Eigen* value of the amplification matrix should not exceed unity. Since the matrix Eq. (28) is triangular, the *Eigen* values are its diagonal elements. The Eigen values of the amplification matrix are $(1 - I)/(1 + I)$, $(1 - J)/(1 + J)$ and $(1 - L)/(1 + L)$.

Assuming that, u is everywhere non-negative and v is everywhere non-positive, we get

$$I = 2\frac{\Delta t}{(y)^2}\sin^2\left(\frac{\beta\Delta y}{2}\right) + \frac{(M + K^{-1})}{2}\Delta t.$$

Since the real part of A is greater than or equal to zero, $|(1 - I)/(1 + I)| \leqslant 1$ always. Similarly, $|(1 - J)/(1 + J)| \leqslant 1$ and $|(1 - L)/(1 + L)| \leqslant 1$. Hence, the finite difference scheme is unconditionally stable. The local truncation error is $O(\Delta t^2 + \Delta y^2)$ and it tends to zero as Δt and Δy tend to zero. Hence, the scheme is compatible. Stability and compatibility ensures convergence.

5.2. Accuracy

We have obtained a comprehensive range of solutions to the transformed conservation equations. To test the validity of numerical Crank Nicolson computations, we have compared the flow velocity and Concentration distributions in Tables 1 and 2 with the Laplace transform solutions. It is clearly seen from Tables 1 and 2 that the results are in excellent agreement. As the accuracy of the numerical solutions is very good, the values of u and ϕ corresponding to analytical and numerical solutions are very close to each other. Table 1 shows that the flow velocity is found to accelerate with Grashoff number for mass transfer Gr_m from 0.0 through 5.0 to 10.0. On the other hand, increasing the Schmidt number Sc from 0.30 through 0.60 to 0.78 the Concentration distribution is found to depress asymptotically throughout the motion (Table 2).

6. Results and discussion

To gain a perspective of the physics of the flow regime, we have numerically evaluated the effects of Hartmann number (M), Grashoff number (Gr), radiation-conduction parameter (R), dimensionless time (t) and porosity parameter (K), on the velocity, u, temperature, θ, concentration, ϕ, shear stress function, τ. Here we consider $Gr = 5 = Gr_m > 0$ (cooling of the plate) i.e. free convection currents convey heat away from the plate into the boundary layer and $t = 0.5R = 10$ throughout the discussion. Also the values of the Schmidt number (Sc), as chosen to represent the presence of various species Hydrogen ($Sc = 0.20$, hydrogen gas diffusing in electrically-conducting air), Helium ($Sc = 0.30$), Steam ($Sc = 0.60$) and Oxygen ($Sc = 0.66$). The Prandtl number Pr is taken for air at 20 °C ($Pr = 0.71$), electrolytic solution ($Pr = 1.0$) and water ($Pr = 7.0$). To ascertain the accuracy of the numerical results, the present study is compared with the previous study. The velocity and concentration profiles are compared with the available solutions of Jaiswal and Soundalgekar [4], and Kumar and Verma [8]. It is observed that the present results are in good agreement with those of [4,8].

Fig. 2 reveals the effects of t and Pr on the transient velocity profiles. It is evident from the figure that the velocity increases with an increase in time for both air and water. Furthermore, the velocity increases and attains its maximum value in the vicinity of the plate and then fades away. The magnitude of velocity for $Pr = 0.71$ is much higher than that of $Pr = 1$ and $Pr = 7$. Physically, this is possible because fluids with high Prandtl numbers have high viscosity and hence move slowly that is smaller values of Pr are equivalent to increasing the thermal conductivity, and therefore heat is able to diffuse away from the heated surface more rapidly than of higher values of Pr. These results agree with the earlier results of Ahmed [6].

Fig. 3 reveals the effects of K on the velocity profiles. The presence of a porous medium increases the resistance to flow resulting in decrease in the flow velocity. This behavior is depicted by the decrease in the velocity as K decreases for both air and water. The magnitude of velocity for air is higher than that of water. This result also corresponds to those of Jaiswal and Soundalgekar [4] and Zueco [9].

Fig. 4 concerns with the effect of Sc and time parameter t on the concentration ϕ. It is noted that the concentration at all points in the flow field decreases exponentially with y and

Table 1 Comparison of values of the *flow velocity* (u) for the present results (*Laplace Technique and Crank Nicolson Method*) with $Gr = 5$, $R_a = 2$, $K = 0.2$, $Sc = 0.78$, $M = 5.0$, $t = 0.5$ and $Pr = 0.71$.

	Laplace technique			Crank Nicolson method		
	Gr_m			Gr_m		
y	0.0	5.0	10.0	0.0	5.0	10.0
0.0	1	1	1	1	1	1
2.0	4.753145	5.258217	5.847471	4.754853	5.258926	5.847614
4.0	0.517363	1.242051	1.507921	0.518530	1.242217	1.507975
6.0	0.085017	0.087154	0.098052	0.085206	0.087246	0.098102
8.0	0.006413	0.008183	0.009453	0.006537	0.008231	0.009573
10.0	0.000861	0.000981	0.002614	0.000872	0.000989	0.002715

Table 2 Comparison of values of the concentration (ϕ) for the present results (*Laplace Technique and Crank Nicolson Method*) with $t = 1.5$, $C_r = 1$.

	Laplace technique			Crank Nicolson method		
	Sc			Sc		
y	0.30	0.60	0.78	0.30	0.60	0.78
0.0	1.000000	1.000000	1.000000	1.000000	1.000000	1.000000
2.0	0.347031	0.317402	0.284172	0.348051	0.317541	0.284308
4.0	0.118063	0.075043	0.038730	0.118131	0.075170	0.038855
6.0	0.024571	0.006527	0.002743	0.024618	0.006617	0.002782
8.0	0.003620	0.001209	0.000451	0.003704	0.001314	0.000507
10.0	0.000852	0.000372	0.000085	0.000867	0.000383	0.000091

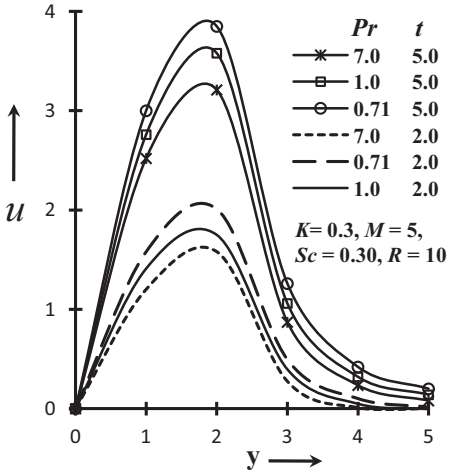

Figure 2 Velocity distributions for Pr and t.

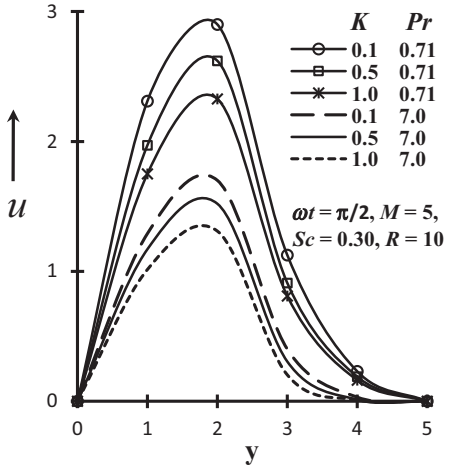

Figure 3 Velocity distributions for Pr and K.

tends to zero as $y \to 5$. A comparison of curves in the figure shows a decrease in concentration with an increase in Schmidt number. Physically it is true, since the increase of Sc means decrease of molecular diffusivity and therefore decrease in concentration boundary layer. Hence, the concentration of species is higher for small values of Sc and lower for large values of Sc. On the other hand, it is found to escalate the concentration with time.

Fig. 5 reveals the transient temperature profiles against y (distance from the plate). The magnitude of temperature is maximum at the plate and then asymptotically decays to zero. The magnitude of temperature for air ($Pr = 0.71$) is greater than that of water ($Pr = 7$). This is due to the fact that thermal conductivity of fluid decreases with increasing Pr, resulting in a decrease in thermal boundary layer thickness. The temperature falls with an increase in the time parameter t for both air and water.

The effect of conduction-radiation parameter, R (i.e. stark number) on the velocity and temperature variations along the vertical surface i.e. in the stream wise direction is depicted in Fig. 6(a) and (b). As R increases, considerable reduction is observed in velocity and temperature profiles from the peak value at the wall ($y = 0$) across the boundary layer regime to the free stream, at which the velocity and temperature are negligible for any value of R. It is also observed that reduction in velocity and temperature is accompanied by simultaneous

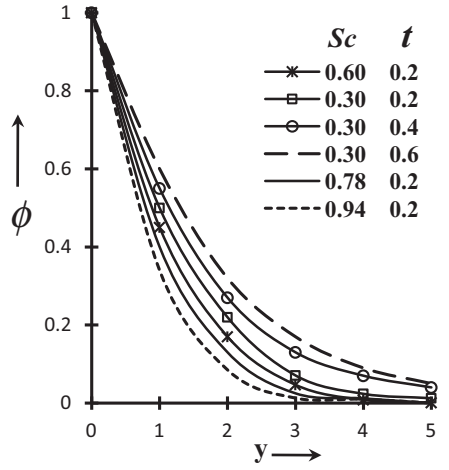

Figure 4 Concentration profiles for *Sc* and *t*.

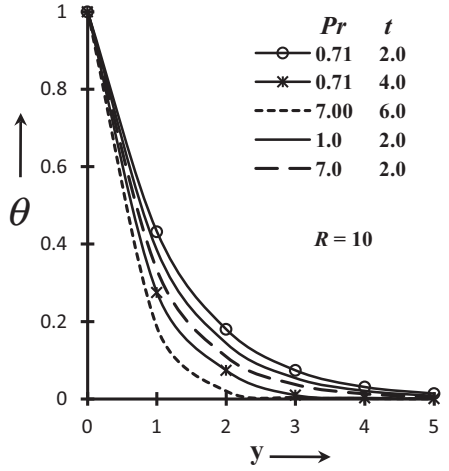

Figure 5 Temperature profiles for *Pr* and *t*.

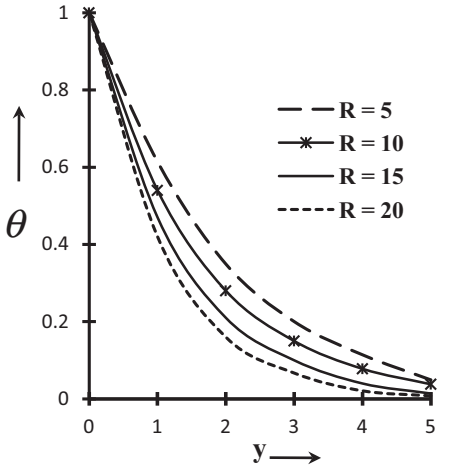

Figure 6 *(continued)*

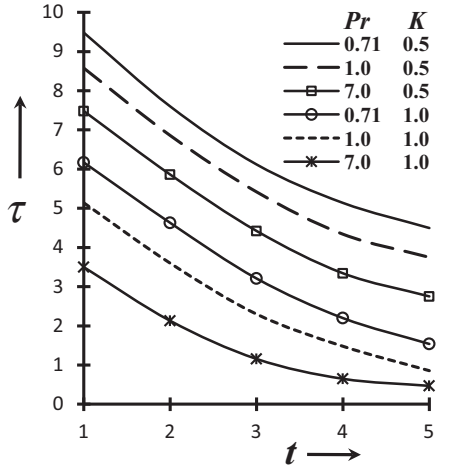

Figure 7 (a) Shear stress for *Pr* and *K* and (b) shear stress for *M*.

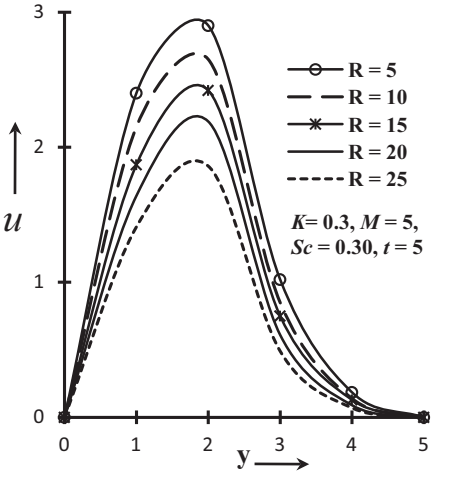

Figure 6 (a) Velocity profiles for *R* and (b) temperature profiles for *R*.

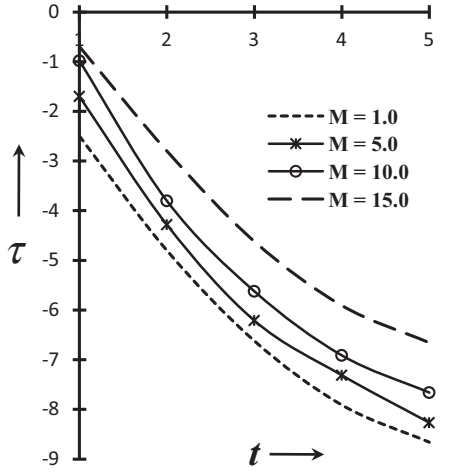

Figure 7 (*continued*)

reductions in both velocity and thermal boundary layers. All pro files decay asymptotically to zero in the free stream. This is in accordance with the results of Raptis and Perdikis [13] and Mahmoud–Chamkha [10].

Fig. 7(a) and (b) reveals the skin-friction against time t for various values of parameters M and K. It is observed that as time passes the skin friction decreases, but it decreases with M due to the pull of Lorentz force, this serves to decelerate the flow along the plate. The skin-friction decreases with increasing permeability parameter K for both air and water. The magnitude of the skin-friction for water is greater than that for air ($Pr = 0.71$) and electrolytic solution ($Pr = 1.0$).

7. Conclusions

Transient free convection-radiation magnetohydrodynamic viscous flow along an infinite vertical permeable plate immersed in a porous medium under a transverse magnetic field has been presented. A flux model has been employed to simulate thermal radiation effects, valid for optically-thick gases. Analytical solutions through Laplace Technique have been obtained for the non-dimensionalized conservation equations, under appropriate boundary conditions and the results indicate that:

- The flow is generally decelerated with the increase of porosity parameter (K) for both the cases of air and water. Temperatures are also depressed with increasing K.
- With an increase in time (t), the flow is progressively accelerated, while temperatures elapse with time.
- Velocity and temperature were decreased with an increase in free convection-radiation (R).
- Increasing porosity contribution (K) serves to depress shear stress significantly in the regime for both the cases of air and water.
- With an increase in time (t), the flow is progressively accelerated and temperatures are depressed.

The current study has employed a Newtonian viscous model. Presently the authors are extending this work to consider viscoelastic fluids and also power-law rheological fluids. The results of these studies will be presented in our next articles.

References

[1] A. Raptis, N.G. Kafoussias, Magnetohydrodynamic free convection flow and mass transfer through porous medium bounded by an infinite vertical porous plate with constant heat flux, Can. J. Phys. 60 (12) (1982) 1725–1729.

[2] M.A. Sattar, Unsteady hydromagnetic free convection flow with Hall current mass transfer and variable suction through a porous medium near an infinite vertical porous plate with constant heat flux, Int. J. Energy Res. 17 (1993) 1–5.

[3] Y.J. Kim, Heat and mass transfer in MHD micropolar flow over a vertical moving porous plate in a porous medium, Transp. Porous Media 56 (1) (2004) 17–37.

[4] B.S. Jaiswal, V.M. Soundalgekar, Oscillating plate temperature effects on a flow past an infinite vertical porous late with constant suction and embedded in a porous medium, Heat Mass Transfer. 37 (2001) 125–131.

[5] A. Raptis, C. Perdikis, Unsteady flow through a highly porous medium in the presence of radiation, Transp. Porous Media 57 (2004) 171–179.

[6] S. Ahmed, Transient three dimensional flow through a porous medium with transverse permeability oscillating with time, Emirate J. Eng. Res. 13 (2008) 11–17.

[7] S. Ahmed, Free convective transient three-dimensional flow through a porous medium oscillating with time in presence of periodic suction velocity, Int. J. Appl. Math. Mech. 6 (2010) 1–16.

[8] A.G.V. Kumar, S.V.K. Verma, Thermal radiation and mass transfer effects on MHD flow past a vertical oscillating plate with variable temperature effects variable mass diffusion, Int. J. Eng. 3 (2011) 493–499.

[9] J. Zueco, Unsteady free convection-radiation flow over a vertical wall embedded in a porous medium, Commun. Numer. Methods Eng. 24 (2008) 1093–1105.

[10] A.A. Mahmoud, A.J. Chamkha, Non-similar solutions for heat and mass transfer from a surface embedded in a porous medium for two prescribed thermal and solutal boundary conditions, Int. J. Chem. Reactor Eng. 8 (2010) 1–24.

[11] V.M. Soundalgekar, H.S. Takhar, Radiation effects on free convection flow past a semi-infinite vertical plate, Model. Meas. Control B 51 (1993) 31–40.

[12] M.A. Hossain, H.S. Takhar, Radiation effect on mixed convection along a vertical plate with uniform surface temperature, Heat Mass Transfer. 31 (1996) 243–248.

[13] A. Raptis, C. Perdikis, Radiation and free convection flow past a moving plate, Int. J. Appl. Mech. Eng. 4 (1999) 817–821.

[14] S. Ahmed, Induced magnetic field with radiating fluid over a porous vertical plate: analytical study, J. Naval Archit. Mar. Eng. 7 (2010) 83–94.

[15] S. Ahmed, Mathematical model of induced magnetic field, with viscous/magnetic dissipation bounded by a porous vertical plate in presence of radiation, Int. J. Appl. Math. Mech. 8 (1) (2012) 86–104.

[16] S. Ahmed, K. Kalita, A sinusoidal fluid injection/suction on MHD three-dimensional Couette flow through a porous medium in the presence of thermal radiation, J. Energy Heat Mass Transfer 35 (2012) 41–67.

[17] S. Ahmed, K. Kalita, Magnetohydrodynamic transient flow through a porous medium bounded by a hot vertical plate in presence of radiation: a theoretical analysis, J. Eng. Phys. Thermophys. 86 (1) (2012) 31–39.

[18] S. Ahmed, K. Kalita, Analytical and numerical study for MHD radiating flow over an infinite vertical plate bounded by porous medium in presence of chemical reaction, J. Appl. Fluid Mech. 6 (4) (2013) 597–607.

[19] S. Ahmed, J. Zueco, L.M. López-Ochoa, Numerical modeling of MHD convective heat and mass transfer in presence of first order chemical reaction and thermal radiation, Chem. Eng. Commun. 201 (3) (2014) 419–436, http://dx.doi.org/10.1080/00986445.2013.775645.

[20] S. Ahmed, A. Batin, A.J. Chamkha, Finite difference approach in porous media transport modeling for magnetohydrodynamic unsteady flow over a vertical plate: Darcian model, Int. J. Numer. Methods Heat Fluid Flow 24 (5) (2014) 1204–1223, 10.1108/HFF-01-2013-0008.

[21] S. Ahmed, Numerical analysis for magnetohydrodynamic chemically reacting and radiating fluid past a non-isothermal impulsively started vertical surface adjacent to aporous regime, Ain Shams Eng. J. 5 (2014) 923–933, http://dx.doi.org/10.1016/j.asej.2014.02.005.

[22] B. Carnahan, H.A. Luther, J.O. Wilkes, Applied Numerical Methods, John Wily and Sons, New York, 1969.

[23] S. Kumar, A new fractional modelling arising in Engineering Sciences and its analytical approximate solution, Alexandria

Eng. J. 52 (4) (2013) 813–819, http://dx.doi.org/10.1016/j.aej.2013.09.005.

[24] R. Ellahi, M. Hameed, Numerical analysis of steady non-Newtonian flows with heat transfer analysis, MHD and nonlinear slip effects, Int. J. Numer. Methods Heat Fluid Flow 22 (1) (2012) 24–38, http://dx.doi.org/10.1108/09615531211188775.

[25] R. Ellahi, E. Shivanian, S. Abbasbandy, S.U. Rahman, T. Hayat, Analysis of steady flows in viscous fluid with heat transfer and slip effects, Int. J. Heat Mass Transfer 55 (23–24) (2012) 6384–6390, http://dx.doi.org/10.1016/j.ijheatmasstransfer.2012.06.026.

[26] S. Ahmed, O.A. Bég, S.K. Ghosh, A couple stress fluid modeling on free convection oscillatory hydromagnetic flow in an inclined rotating channel, Ain Shams Eng. J. 5 (2014) 1249–1265, http://dx.doi.org/10.1016/j.asej.2014.04.006.

[27] J. Zueco, S. Ahmed, L.M. López-Ochoa, Magneto-micropolar flow over a stretching surface embedded in a Darcian porous medium, Arab. J. Sci. Eng., 2014. http://dx.doi.org/10.1007/s13369-014-1175-7 (in press).

[28] F.S. Ibrahim, A.M. Elaiw, A.A. Bakr, Effect of the chemical reaction and radiation absorption on the unsteady MHD free convection flow past a semi infinite vertical permeable moving plate with heat source and suction, Commun. Nonlinear Sci. Numer. Simul. 13 (2008) 1056–1066, http://dx.doi.org/10.1016/j.cnsns.2006.09.007.

[29] D. Pal, B. Talukdar, Influence of fluctuating thermal and mass diffusion on unsteady MHD buoyancy-driven convection past a vertical surface with chemical reaction and Soret effects, Commun. Nonlinear Sci. Numer. Simul. 17 (2012) 1597–1614, http://dx.doi.org/10.1016/j.cnsns.2011.08.038.